RSC Advances

PAPER

View Article Online
View Journal | View Issue

Cite this: *RSC Adv.*, 2021, **11**, 12696

The optical shielding performances and mechanisms of green flame-retardant two-component matte films under various application conditions

Xuan Yin [abc] and Yunjun Luo [*b]

Received 16th February 2021
Accepted 18th March 2021

DOI: 10.1039/d1ra01266e

rsc.li/rsc-advances

Herein, we meticulously investigated the optical shielding performances and mechanisms of green flame-retardant two-component waterborne polyurethane matte films based on a previous study. The relevant performances were evaluated by changing various environmental factors including nanoparticle content, pH, temperature and storage-time. Specifically, upon combination with TiO_2, the ultraviolet-light transmittance was reduced to 1.9% and the 60° glossiness decreased by 63%. When the pH was 8.0, the shielding efficiency and transmittance of ultraviolet light were 100% and 0%, respectively. The 60° glossiness of spin-films increased with an increase in storage time. Besides, TiO_2 nanoparticles were beneficial for delaying the thermal decomposition *via* synergistic flame retardance.

Introduction

The common application areas of coatings include buildings, textiles, wood and leather, especially flammable textiles and wood. Hence, the modification of the flame retardance of coatings that are applied in textiles and wood is important.[1–3] Flame retardants vary depending on their molecular structure, chemical components and physical properties. Among the applied types of flame retardants, halogen-free flame retardants have been widely used in the modification of waterborne polyurethanes. Previously, the main waterborne polyurethanes are one-component waterborne polyurethanes, which have many advantages, and thus are widely applied. However, one-component waterborne polyurethanes lack excellent chemical resistance, hardness and mechanical performances.[4,5] Therefore, two-component waterborne polyurethanes (2K-WPUs) have been developed to address these problems.[6,7] The 2K-WPUs consist of an aqueous hydroxyl component and polyisocyanate component, which have the advantages of both solvent-based polyurethane coatings and water-based coatings.[8,9] At present, several trends have been observed for 2K-WPUs. Firstly, synergistic flame retardance not only significantly maintains flame retardancy but also expands the application of various flame retardant elements[10,11] and flame retardant mechanisms.[12,13] Secondly, according to requirements, the ideal-functionalized 2K-WPU has multi-functions such as matte appearance,[14,15] fluorescence,[16] specular reflection[7] and anti-corrosion properties.[17,18] Thirdly, compared to non-flame-retardant 2K-WPUs, the thermostability, mechanical performance and water-resistance of flame retardant 2K-WPUs are slightly inadequate due to the combination of flame retardants.[13,19] Hence, the choice of an appropriate matrix or raw materials is crucial for improving system performances, which makes it easy to achieve practical requirements for 2K-WPUs.

Aiming at functionalized 2K-WPUs, shielding ultraviolet light is one of the goals for multi-functionalization. To shield ultraviolet light, materials must absorb or reflect ultraviolet light to weaken its transmission ability.[8,20] Generally, 2K-WPUs have high glossiness without shielding ultraviolet light. However, in some special conditions (*i.e.*, outdoors), the large surfaces of textile materials and wooden furniture cannot reflect or shield ultraviolet light and visible light.[21] According to different wavelengths, ultraviolet light is divided into the shortwave region (190–280 nm), mediumwave region (280–320 nm) and longwave region (320–400 nm). Ultraviolet light within the mediumwave region and longwave region is very harmful to the human body,[22] while xylogen in wood materials is easily degraded by irradiation from ultraviolet light in the shortwave and mediumwave regions, causing wood to be damaged.[23] When the human body and woodware are exposed to ultraviolet radiation, their non-modified surfaces cannot protect them.[24] Therefore, it is crucial to research optical shielding 2K-WPUs for protecting textile materials and wooden furniture.

In our previous paper, titanium dioxide (TiO_2) nanoparticles tremendously improved the mechanical properties and flame resistance of green flame-retardant 2K-WPUs.[25,26] Meanwhile, the green flame-retardant two-component waterborne

[a]*College of Mechanical and Electrical Engineering, Beijing University of Chemical Technology, Beijing 100029, China*
[b]*Beijing Institute of Technology, Beijing 100081, China. E-mail: yjluo@bit.edu.cn*
[c]*Tsinghua University, Beijing 100084, China*

polyurethane matte films exhibited good flame retardance, where all the films achieved an oxygen index of over 29.4% and V-0 level of UL-94. In contrast, herein, we mainly characterized and analyzed the influence of environment elements (including pH, temperature, and storage time) on the optical shielding in detail. These discoveries will afford effective guidance to design the structure of green flame-retardant two-component waterborne polyurethane matte films based on nanoparticles and broaden the applications of flame-retardant two-component waterborne polyurethane matte films in practical conditions such as surface engineering and coating industry.

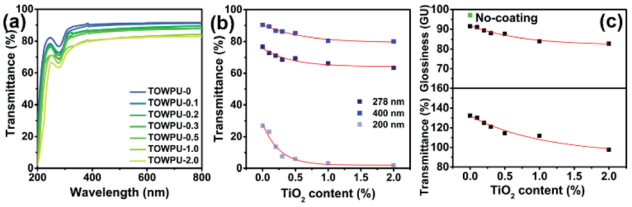

Fig. 2 Analysis of the optical shielding performances for the spin films affected by TiO_2 content. (a) Ultraviolet spectra of the emulsion. (b) Ultraviolet-light transmittance curves of the emulsion at various wavelengths. (c) 60° glossiness curves of spin films and visible light transmittance of the emulsion. The variations in the point diagrams are marked as light red color curves and fitted by Gaussian fitting.

Results and discussion

TiO_2 content

In previous research, the results indicated that the gain size increases with an increase in TiO_2 content. The detailed size distribution curves are shown in Fig. 1. As shown in Fig. 1a, the peaks of the size distribution appear at 1.0 wt%, and three peaks appear at 2.0 wt%. A higher nanoparticle content resulted in agglomeration to produce larger nanoparticles, which tremendously affected the size distribution. Fig. 1b shows the change in the size distribution and successful synthesis of the specimens. Therefore, under the influence of various factors, the optical performances and shielding mechanism of the TOWPU system were thoroughly analyzed and discussed.

According to previous research (Fig. 2a), the ultraviolet transmittance always decreases with an increase in TiO_2 content,[26] which is caused by the following two reasons. Generally, ultraviolet transmittance represents the optical shielding performances, which can be analyzing by measuring the emulsion and spin films. On the one hand, there is a large number of chromophores containing non-bonding electrons (C=O groups containing n electrons) and chromophores containing antibonding electrons (six-membered heterocyclic nitrogen containing π* electrons originating from the curing agent molecular chains of polyurethane cross-linking network) in the cross-linking network. Under the excitation of ultraviolet light, the n → π* electron transfers from the C=O groups to the six-membered heterocyclic nitrogen. In this case, with the addition of TiO_2, the ultraviolet spectrum of the TOWPU spin films exhibits an ultraviolet absorption peak stimulated by the n → π* electron transfer.[27] On the other hand, shielding of ultraviolet light strengthened by the shifted and highly reactive electron–hole pairs is also a reason. The electronic structure of TiO_2 consists of a valence band and conduction band formed by the lowest unoccupied molecular orbital (LUMO). The electronic structure of TiO_2 can absorb the larger energy of light than the energy gap when TiO_2 nanoparticles are irradiated by ultraviolet light, and thus the electrons in the valence band are excited to the conduction band. Consequently, the hole formed due to a lack electrons in the valence band is easily shifted. Also, these highly reactive electron–hole pairs strengthen the shielding of ultraviolet light.[28,29]

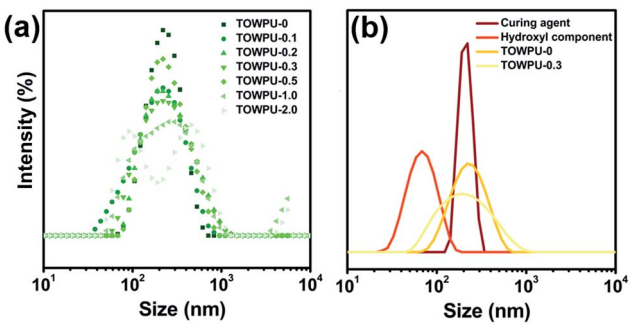

Fig. 1 Emulsion performances of TOWPU system. (a) Emulsion particle distribution curve. (b) Comparison of the emulsion particle distribution curve among two types of components and TOWPU systems.

To deeply research the variation, we considered different wavelengths (200 nm, 278 nm, and 400 nm) as sampling points. As shown in Fig. 1b, the ultraviolet transmittance decreased with an increase in TiO_2 content, especially in the near ultraviolet region (190–280 nm). The first reason leading to this change is the addition of more TiO_2 nanoparticles enhances the ability to absorb and reflect ultraviolet light. Under this condition, the system produces higher activity and electron–hole pair mobility under stronger shielding. Conversely, based on the covalent bond of the chemical cross-linked network formed by the –OH and –NCO groups, more TiO_2 can also produce excited C=O chromophores and electron–hole pairs on the molecular chains. This reaction also increases the shielding performance of the system, specifically, a form of matte film with capability to reflect natural light and obtain low glossiness. Meanwhile, given that the ultraviolet region and infrared region are included in the wavelength coverage of natural light, the optical shielding ability of spin films is equal to the reflectivity of ultraviolet and infrared light, characterizing the 60° glossiness, as shown in Fig. 2c. This section is also reported in the previous research.[26] Comparing Fig. 1 with Fig. 2, the larger gain size of TiO_2 nanoparticles and greater content both promoted a more remarkable reduction in 60° glossiness (from 154.2 to 97.6) for the spin films. Also, higher reflectivity was obtained. Moreover, by ruling out the influence of ultraviolet light on the 60° glossiness, the transmittance of natural light was reduced from 91.50% to 82.78% at 760 nm, which is associated with the whiteness and opacity of TiO_2 nanoparticles. It is worth noting

that the characters of TiO_2 are strong coverage and extinction. The former enhances the whiteness of spin films, whereas the latter reduces their opacity. Practically, with these two properties of TiO_2 nanoparticles, the whiteness and opacity of the spin film can be enhanced.

Acid and alkali conditions

At the same pH, the ultraviolet transmittance declined with the addition of TiO_2 nanoparticles, especially when the TiO_2 content was greater than 0.5 wt% (Fig. 3). Because TiO_2 has perfect chemical resistance, it can hardly be affected by alkaline conditions.[30,31] Additionally, a more compact cross-linking network is beneficial to promote the formation of C=O excited chromophores and electron–hole pairs, thus achieving stronger ultraviolet shielding. For simplicity, we choose the TOWPU-0.5 spin film to investigate the optical performances with a change in pH, which are listed in Table 1. When the pH was less than or equal to 6.0, the ultraviolet transmittance declined with a decrease in pH value. Conversely, the ultraviolet transmittance increased with a decrease in pH value when the pH was equal or greater than 7.5. This indicates that our sample displays stronger ultraviolet shielding in an alkaline environment than that in an acidic environment, especially when the pH value is 8.0. Also, this transmittance is lower by 29% when the pH value is 6.0, which is obtained at the ultraviolet absorption peak of 278 nm. Essentially, the abovementioned change is associated with the mass number of positive and negative charges loaded in the side chains of the polymer chain. The acidic environment or alkaline environment provides ionization conditions for the charged groups of 2K-WPUs to a certain degree.[32] Based on the abovementioned synthesis,[26] the polyurethane chains have numerous –COOH groups, which contain negative charges after hydrophilic chain extending of dimethylolpropionic acid. Also, the –COOH groups contain negative charges and the –NH– triethylamine antalkali groups contain positive charges, forming some stable polyurethane chains. In an alkaline environment, particularly when the pH value is equal or greater than 7.5, more positively charged groups increase the number of electron–hole pairs. In this case, the capacity of ultraviolet shielding is improved. In contrast, the ionization of the –COOH groups is induced due to an acid environment with a pH value of no more than 6.0. This reaction influences the chemical resistance of the spin film, which restrains the formation of electron–hole pairs and weak the effect of ultraviolet shielding.

Table 1 Transmittance of the various spin films obtained at different pH

pH	200 nm (%)	278 nm (%)	400 nm (%)
5.5	5.88	69.33	87.4
6.0	17.8	80.1	90
7.0	3	66.3	85.01
7.5	0.5	64.7	80.8
8.0	0	51.1	74.2

Interestingly, the efficiency results of screening ultraviolet and visible light together with a change in pH value were also proven *via* the analysis above, as shown in Fig. 4. As shown in Fig. 4a, the efficiency of screening ultraviolet light in an alkaline environment is higher than that in an acid environment, especially at 8.0 pH (the efficiency of screening ultraviolet light increased from 32.4% to 100% at 200 nm), which is consistent with ultraviolet shielding. Similarly, the 60° glossiness in the alkaline environment was lower than that in the acid environment (less than 100), as shown in Fig. 4b. As mentioned earlier, the acid environment can provide the more positive amino groups to realize more efficient shielding of ultraviolet light, thereby improving the reflectivity of natural light in the spin film. In addition, because its excellent chemical resistance,

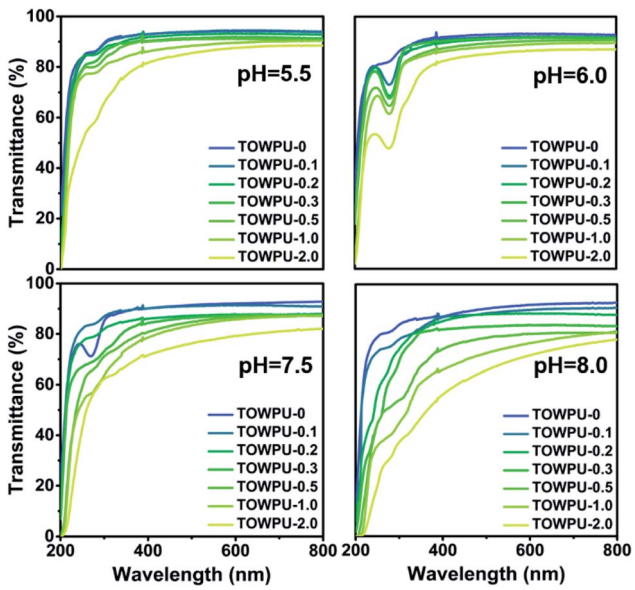

Fig. 3 Ultraviolet spectra of spin films with different pH values.

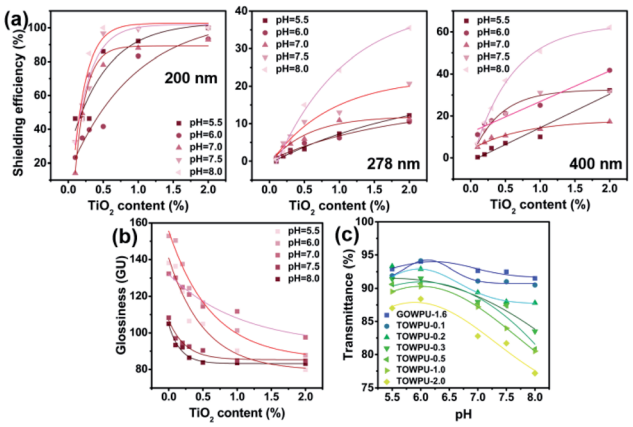

Fig. 4 Shielding efficiency curves of ultraviolet-light of TOWPU-0.5 emulsion affected by pH. (a) Ultraviolet at various wavelengths. (b) 60° glossiness. (c) Visible-light transmittance. The variations in the point diagrams are marked as full color curves and fitted by Gaussian fitting.

a higher content of TiO_2 can delay the variation in 60° glossiness by responding to the pH of the environment. Meanwhile, under the same content of TiO_2, by eliminating the influence of ultraviolet light on the 60° glossiness (Fig. 4c), the transmittance of natural light firstly increased, and then decreased with an increase in pH. This is consistent with the results for ultraviolet shielding.

Temperature

Besides pH, the environmental temperature also had a crucial influence on the optical performances of the emulsion and spin film (Fig. 5). The ultraviolet transmittance declined with an increase in temperature. Because the emulsion particles prevent the light from penetrating the opaque emulsion, the hindered light is scattered on the surface of the emulsion particles. When the temperature increases, the collision among emulsion particles is heightened, which causes the beam of light to scatter more strongly when hitting the emulsion. After the addition of TiO_2 nanoparticles, a change in ultraviolet transmittance was hardly visible. A similar variation was also found for other systems. These results indicate that environmental temperature rarely has an influence on ultraviolet shielding.[29] Meanwhile, the network formed by the –OH groups of the TiO_2 nanoparticles and –NCO groups of the curing agent enlarges the size of the emulsion particles, which causes weaker collision among the emulsion particles to inhibit the light scattering inhibition. The changing trends in the ultraviolet transmittance and efficiency of screening ultraviolet light at different wavelengths are respectively in Fig. 6.

To investigate the effect of temperature on ultraviolet transmittance, the changing trends in ultraviolet transmittance at the wavelengths of 200 nm and 400 nm are shown in Fig. 6a. At the wavelength of 200 nm, all the ultraviolet transmittances are 0, regardless of TiO_2 content and ambient temperature, which indicates that the temperature has an effect on the ability of shielding ultraviolet light in the shortwave region. At the wavelength of 400 nm, and under the same TiO_2 content, the ultraviolet transmittance decreased with heating. Meanwhile, with the addition of TiO_2 nanoparticles, the range of change in the ultraviolet transmittance was smaller. There are two reasons for this change: the abundant TiO_2 and the large size emulsion particles. The former improves the ultraviolet reflectivity of TOWPU, whereas the latter enhances the optical index to reduce ultraviolet light. Furthermore, Fig. 6b shows the efficiency of screening ultraviolet light at the wavelength of 400 nm upon heating. At the same temperature, adding TiO_2 could improve the shielding efficiency. For instance, as the content of TiO_2 nanoparticles increased at 10 °C, the shielding efficiency increased from 60.1% to 80.7%, which is due to the increased reflection and absorption of ultraviolet light. However, with the same TiO_2 content, as the temperature increased, the efficiency

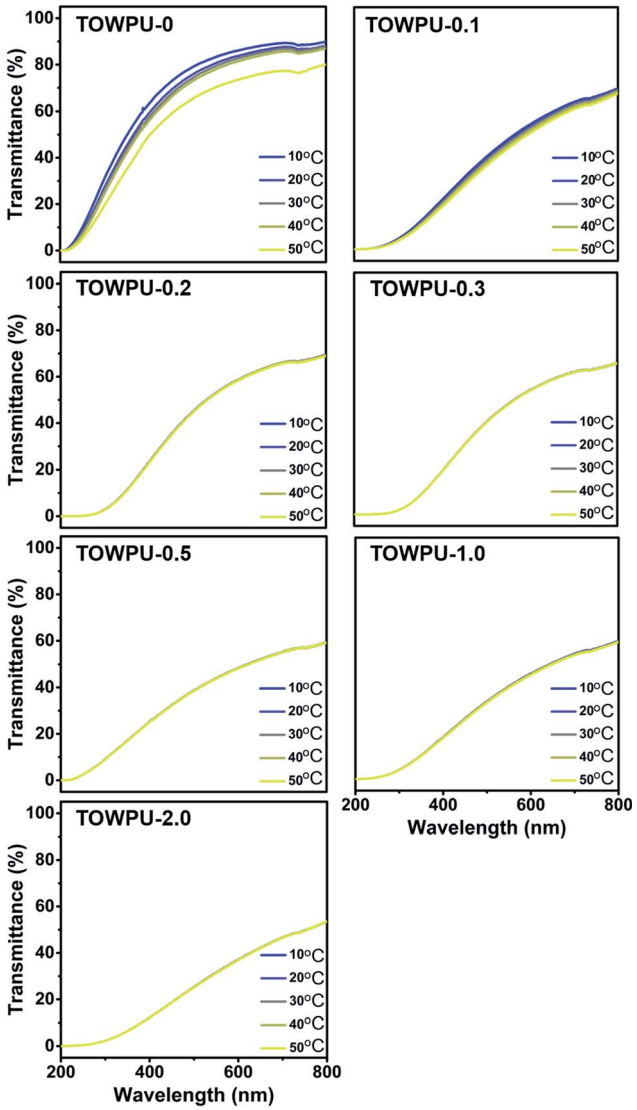

Fig. 5 Ultraviolet spectra of TOWPU emulsion affected by temperature.

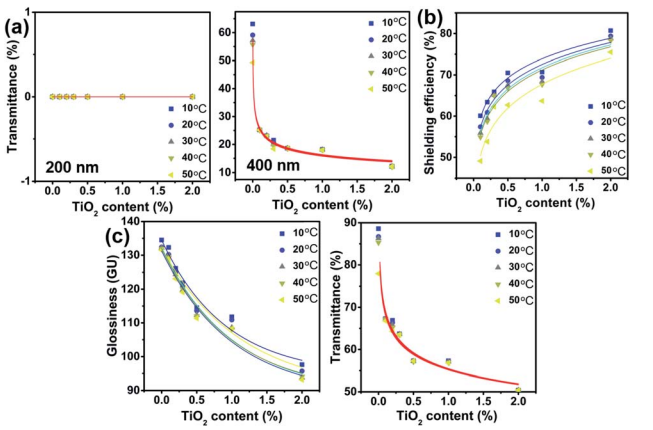

Fig. 6 Changing curves of TOWPU emulsion and its spin films for shielding light. (a) Ultraviolet light transmittance for emulsion at various temperatures. (b) Shielding efficiency of ultraviolet light for emulsion at various temperatures. (c) 60° glossiness and visible light transmittance for spin films at various temperatures. The variations in the point diagrams are marked as red color and the full color curves are fitted by Gaussian fitting.

of screening ultraviolet light decreased. For instance, given that TiO_2 nanoparticles influence the catalytic degradation of 2K-WPU with a change in temperature, the shielding efficiency of TOWPU-0.5 decreased from 70.5% at 10 °C to 62.7% at 50 °C. The effects of the aging actions of TiO_2 on the polymer are three types, namely photodecomposition, photooxidation, and hydrolysis. Therefore, the temperature causes the photo-oxidation of the TiO_2 nanoparticles, which reduces TOWPU, thereby reducing the shielding efficiency. However, considering the close-packed network structure of polyurethane, the content of TiO_2 nanoparticles in the TOWPU system is too small to greatly affect the ability of shielding ultraviolet light. As expected, a similar change was also found in the 60° glossiness of the spin film, which decreased with warming (Fig. 6c). The visible light transmittance (760 nm) of the TOWPU spin film was barely affected by temperature except for the blank control. This result also supports the hypothesis that the content of TiO_2 nanoparticles rarely affects the ability of shielding ultraviolet light *via* photooxidative aging.

Durability

In the applied scenario of production and usage, the durability of emulsions and spin films is also an important index. It was found that the ultraviolet transmittance increased with an increase in storage time in the TOWPU-0.5 specimen, which was caused by two reasons (Fig. 7a). Firstly, the electrons of the forbidden band of TiO_2 nanoparticles leap to the conduction band, which leads to the transfer of electron–hole pairs by absorbing ultraviolet luminous energy. These electron–hole pairs form free radicals with H_2O, oxygen atoms, and hydroxide radical of TiO_2, and thus a photocatalytic reaction is initiated to degrade the polymer.[33,34] Secondly, the molecular structure of the polymer is changed by ultraviolet light, oxygen, heat and humidity. It is worth noting that the maximum content of TiO_2 nanoparticles is 2.0% of solid mass (the solid content of TOWPU is 30%). Therefore, the degradation of TOWPU was hardly incurred by photocatalysis, which can also be verified by the optical performances affected by temperature. Compared with TOWPU-0, due to the ultraviolet resistance of TiO_2 nanoparticles, the influence of ultraviolet transmittance is smaller. In the waterborne polyurethane cross-linking network, the aging of TiO_2 nanoparticles has much lower impact on the performances of TOWPU than its ultraviolet resistance. Consequently, the TiO_2 nanoparticles significantly improved the performances of the spin film.

With an increase in storage time, the 60° glossiness of TOWPU-0 increased by 28, while that of TOWPU-0.5 increased by 2.58 (Fig. 7b). This result indicates that the 60° glossiness of TOWPU is less affected by storage time compared with the blank control specimen. According to the previous investigation, the degradation of TOWPU is weakly incurred by photocatalysis of the TiO_2 nanoparticles. The transmittance of visible light (760 nm) was plotted as a new curve to further investigate the effect of storage time on TOWPU by excluding the ultraviolet effect, as shown in Fig. 4c. Due to weak photodegradation, the shielding efficiency decreased with an increase in storage time. Compared with TOWPU-0, shielding efficiency was generally enhanced, resulting in excellent optical shielding.

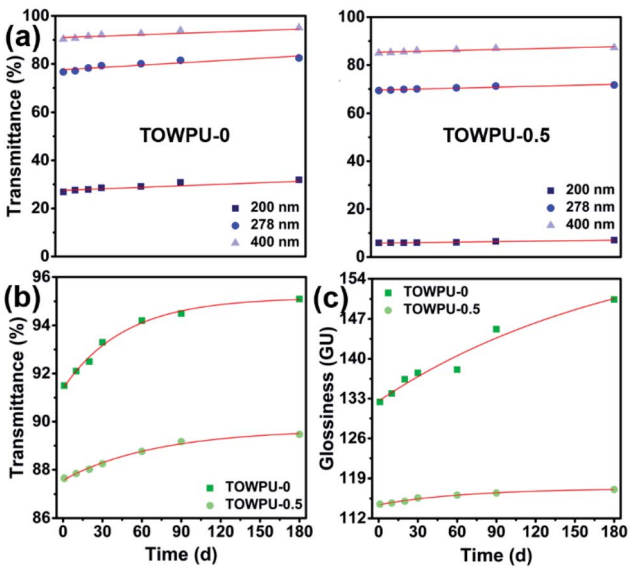

Fig. 7 Optical shielding performances of emulsion and spin films under various storage times. (a) Changing curves of ultraviolet-light transmittance for TOWPU-0 and TOWPU-0.5 emulsion. (b) 60° glossiness curves of TOWPU-0 and TOWPU-0.5 spin films. (c) Visible-light transmittance curves of TOWPU-0 and TOWPU-0.5 spin films. The variations in the point diagrams are marked as light red color curves and fitted by Gaussian fitting.

Flame retardance and mechanism

In our previous work,[26] the limiting oxygen index (LOI) and UL-94 of the TOWPU matte films were 30.0 and V-0 level, respectively. The formative nonflammable carbon layers interrupted the combustion chain reaction to delay combustion. Meanwhile, the TiO_2 nanoparticles could create cladding layers to control the energetic growth, which reduced the energy density and prevented surface heat transmission from combustible gas in the matrix during burning. To further investigate the flame-retardance effect of the TiO_2 nanoparticles, the release rate of pyrolysis gas was characterized by thermogravimetric infrared analysis. Among the six types of TOWPU matte films, TOWPU-0.5 exhibited the best comprehensive performances. Therefore, the TOWPU-0.5 matte film was selected as a representative sample to obtain the flame retardance of the TiO_2 nanoparticles used in the matte film. As shown in Fig. 8, four gas peaks can be visibly observed in the FTIR spectra of TOWPU-0, which are located at 22.6, 29.3, 38.2 and 55.0 min (converting these times to temperatures: 226 °C, 293 °C, 382 °C, and 550 °C, respectively). The locations of the four gas peaks are similar to the weightlessness peaks (Fig. 2 and Table S2 in the previous work[26]). Simultaneously, the peak at 29.3 min is the maximum height. In addition, there is no obvious peak between 40 and 50 min. The reason for this is that the different gases have different photon absorption intensities. Among the released gases in this study, the photon absorption intensities of CO_2 is higher than other gases.[35] The locations of the pyrolysis gas

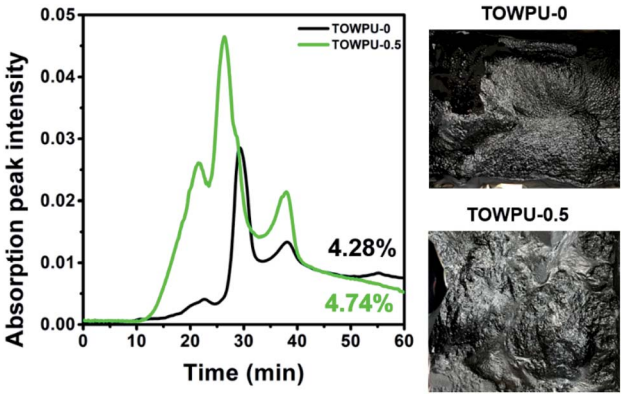

Fig. 8 Flame retardance of matte film. FTIR spectra of pyrolysis gas at 10 °C min^{-1} warming. Images of char residues for TOWPU-0 and TOWPU-0.5 after being tested in air at 500 °C.

peaks at various temperatures are listed in Table 2. The peak observed at 55.0 min is the second peak of the gaseous product in the late stage of thermal decomposition.[36] The FTIR spectrum of TOWPU-0.5 has three obvious gas peaks at 21.7, 26.4 and 37.9 min (converting these times to temperatures: 217 °C, 264 °C, and 379 °C, respectively), which are similar to the corresponding temperatures in the previous work.[26] Similarly, the maximum peak is located at 26.4 min, and there is no obvious peak between 40 and 50 min. However, the second peak for the gaseous product was not detected after 50 min.

Comparing the FTIR spectrum and char residue images of TOWPU-0 and TOWPU-0.5, the gas peak of TOWPU-0.5 is higher because TiO_2 has stronger oxygen catalytic activity in the two-component waterborne polyurethane network. TiO_2 nanoparticles act as a highly active catalytic tank, which can catalyze redox reactions and accelerate thermal decomposition to release gases. After 44.0 min (440 °C), the process occurring is the carbonization of the residue by dehydration. During this process, the intensity of the gas peak in TOWPU-0.5 is significantly lower than that in TOWPU-0. Meanwhile, TOWPU-0.5 has no second gaseous product peak. The TiO_2 nanoparticles were deposited on the surface of the char residues during the entire heating process instead of burning, thereby restraining their thermal decomposition and thermal transmission. This further provides a flame-retardant effect for the systems. Therefore, based on the gas-condensed phase, the TiO_2 nanoparticles act as synergistic flame retardants to insulate heat and inhibit combustion by working with SO_2, polyphosphoric acid and polymetaphosphate acid (the three products derived from the combustion of TOWPU, which are also shown in the previous work[26]).

Table 2 The locations of the pyrolysis gas peaks at various temperatures

Sample	Temperature (°C)	Absorption peak (cm^{-1})	Pyrolysis gas
TOWPU-0	200	2325	HCN
		2365	CO_2
	300	1047	SO_2
		2369	CO_2
	350	928	NH_3
	550	929	NH_3
		2369	CO_2
TOWPU-0.5	200	2320	HCN
		2369	CO_2
	300	1044	SO_2
		2369	CO_2
	350	926	NH_3

Experimental

Materials and methods

The synthesis and basic performances of green flame-retardant 2K-WPUs (named TOWPU, six different TOWPU samples were prepared, with various TiO_2 contents of 0, 0.1, 0.2, 0.3, 0.5 and 1.0 wt%) were recommended in the previous study.[26] Furthermore, herein, we mainly investigated the related characterizations of the optical performances using a laser particle analyzer, ultraviolet spectra and glossiness.

Characterizations

The grain size of the emulsion was measured using a Malvern Zetasizer Nano ZS90 laser particle analyzer at 25 °C for 120 s. Before the measurement, the emulsion was diluted to 1.0 wt% with deionized water. A U-3010 Hitachi ultraviolet-visible spectrophotometer was utilized to test the emulsion on quartz plates by scanning in the wavelength range of 200 to 800 nm. There were two types of tested specimens, one was spin films, specifically, where the emulsion was spun on the surface of a 25 × 25 mm^2 quartz plate and then dried at 60 °C in a vacuum oven before the testing, and the other one was a diluted solution (the original emulsion was diluted 1000 times), which was placed in a 10 × 10 × 50 mm^3 quartz cuvette. A Ref101N-min 60° glossmeter was utilized to test the natural light shielding in the spin films. The spin films were prepared by spinning the original emulsion on a 25.6 × 72.4 × 2 mm^3 glass slide, and then drying at 60 °C in a vacuum oven for 12 h. According to Japanese Industrial Standards (JIS), the refractive index and reflectivity of a black glass surface are 1.567% and 10%, respectively, and are defined as 100.0 CU at a 60° angle of incidence. The 60° glossiness based on the glass slide was larger than 100.0 CU. In addition to the optical performances measured in an ordinary environment by changing the TiO_2 content, other special application conditions were set and tested as follows. For acid and alkali conditions (the influence of pH), the emulsion or spin-films were immersed in acid or lye for 12 h and tested immediately. For temperature-changing environment, the emulsion or spin films were placed in a vacuum drying oven at various temperatures for 2 h and tested immediately. For durability with an increase in storage time, the emulsion was set under ordinary conditions. The gaseous products from the thermal degeneration of the TOWPU matte films were tested *via* thermogravimetric infrared analysis (Mettler Toledo TGA/DSC1-Nicolet 6700 FTIR) under the condition of 30 °C to 500 °C in

nitrogen at a heating rate 10 °C min^{-1}. Also, the matte films were burned to obtain the char radius at 500 °C in air.

Conclusions

With an increase in TiO_2 content, the ultraviolet transmittance and 60° glossiness of system always decreased. In an alkaline environment, the efficiency of ultraviolet shielding (100%) was stronger than that in an acid environment due to the larger number of electron–hole pairs. Furthermore, the glossiness increased with an increase in storage time. The network formed by the –OH groups of the TiO_2 nanoparticles and –NCO groups of the curing agent enlarged the size of the emulsion particles, which caused weaker collisions among the emulsion particles to inhibit the light scattering inhibition. In addition, the TiO_2 nanoparticles were beneficial for delaying thermal decomposition to enhance the flame retardance of SO_2, polyphosphoric acid and polymetaphosphate acid. These results provide guidance for simulating and applying waterborne polyurethane matte films under broader conditions.

Author contributions

Y. L. conceived the idea and designed the experiments. X. Y. synthesized the samples, performed all the experiments and data analysis. All authors contributed to the writing of the manuscript.

Conflicts of interest

There are no conflicts to declare.

Acknowledgements

This work is funded by the National Natural Science Foundation of China under Grant No. 51905295, and the National Key Research and Development Program of China under Grant No. 2016YFC0204400.

Notes and references

1 X. Li, N. Liu, J. Hao, M. Dun and W. Wang, *Journal of Forestry Engineering*, 2020, **5**, 80–88.
2 Q. Tang, L. Fang and W. Guo, *Journal of Forestry Engineering*, 2020, **5**, 87–92.
3 M. Zhu, C. Ding, S. Zhang and Y. Huang, *Journal of Forestry Engineering*, 2020, **5**, 1–12.
4 C. Shao, J. Huang, G. Chen, J. Yeh and K. Chen, *Polym. Degrad. Stab.*, 1999, **65**, 359–371.
5 M. Martin, S. Michae, K. Claus and J. Eberhard, *Prog. Org. Coat.*, 2000, **40**, 99–109.
6 Z. Ge and Y. Luo, *Prog. Org. Coat.*, 2013, **76**, 1522–1526.
7 X. Yin, B. Zhang and Y. Luo, *Polym. Sci., Ser. B*, 2018, **59**, 697–707.
8 S. Bhargava, M. Kubota, R. D. Lewis, S. G. Advani, A. K. Prasad and J. M. Deitzel, *Prog. Org. Coat.*, 2015, **79**, 75–82.
9 X. Yong, Y. Song, Y. Wang and M. Zhang, *Prog. Org. Coat.*, 2014, **77**, 1972–1976.
10 Y. Liu, *Polymer*, 2001, **42**, 3445–3454.
11 M. Chen, Z. Shao, X. Wang, L. Chen and Y. Wang, *Ind. Eng. Chem. Res.*, 2012, **51**, 9769–9776.
12 J. Hu and F. Zhang, *J. Therm. Anal. Calorim.*, 2014, **118**, 1561–1568.
13 B. Yu, Y. Shi, B. Yuan, S. Qiu, W. Xing, W. Hu, L. Song, S. Lo and Y. Hu, *J. Mater. Chem. A*, 2015, **3**, 8034–8044.
14 J. Uribe-Padilla, M. Graells-Sobré and J. Salgado-Valle, *Prog. Org. Coat.*, 2017, **109**, 179–185.
15 Q. Yong, F. Nian, B. Liao, Y. Guo, L. Huang, L. Wang and H. Pang, *Polym. Bull.*, 2016, **74**, 1061–1076.
16 X. Yin, X. Li and Y. Luo, *Polymers*, 2017, **9**, 492–506.
17 K. Zhu, X. Li, H. Wang, J. Li and G. Fei, *J. Appl. Polym. Sci.*, 2017, **134**, 44445.
18 T. Pan and Q. Yu, *J. Mater. Eng. Perform.*, 2016, **25**, 2384–2394.
19 W. Cai, J. Zhan, X. Feng, B. Yuan, J. Liu, W. Hu and Y. Hu, *Ind. Eng. Chem. Res.*, 2017, **56**, 7229–7238.
20 X. Wang, S. Zhou and L. Wu, *Mater. Chem. Phys.*, 2012, **137**, 644–651.
21 T. T. X. Hang, N. T. Dung, T. A. Truc, N. T. Duong, B. V. Truoc, P. G. Vu, T. Hoang, D. T. M. Thanh and M.-G. Olivier, *Prog. Org. Coat.*, 2015, **79**, 68–74.
22 S. Seyed, I. Seyed, J. Kong and X. Lu, *ACS Sustainable Chem. Eng.*, 2017, **5**, 3148–3157.
23 M. Nikolic, J. M. Lawther and A. R. Sanadi, *J. Coat. Technol. Res.*, 2015, **12**, 445–461.
24 S. M. Fufa, B. P. Jelle and P. J. Hovde, *Prog. Org. Coat.*, 2013, **76**, 1425–1429.
25 X. Yin, C. Dong and Y. Luo, *Colloid Polym. Sci.*, 2017, **295**, 2423–2431.
26 X. Yin, C. Dong, C. Chai and Y. Luo, *Prog. Org. Coat.*, 2018, **122**, 119–128.
27 S. Qiu, F. Deng, S. Xu, P. Liu, X. Min and F. Ma, *J. Wuhan Univ. Technol.*, 2015, **30**, 447–451.
28 Y. Wen, S. Liu, Q. Zhang, Y. Zhang, Z. Yang and A. Zhu, *Mater. Lett.*, 2016, **163**, 262–265.
29 P. Chen, *Mater. Lett.*, 2016, **163**, 130–133.
30 X. H. Hu, X. Y. Zhang and J. B. Dai, *Chin. Chem. Lett.*, 2011, **22**, 997–1000.
31 X. Hu, X. Zhang, J. Dai and J. Liu, *J. Lumin.*, 2011, **31**, 2160–2165.
32 V. G. Nguyen, H. Thai, D. H. Mai, H. T. Tran, D. L. Tran and M. T. Vu, *Composites, Part B*, 2013, **45**, 1192–1198.
33 M. Vlad Cristea, B. Riedl and P. Blanchet, *Prog. Org. Coat.*, 2010, **69**, 432–441.
34 T. V. Nguyen, P. H. Dao, K. L. Duong, Q. H. Duong, Q. T. Vu, A. H. Nguyen, V. P. Mac and T. L. Le, *Prog. Org. Coat.*, 2017, **110**, 114–121.
35 G. Li, W. Lei, H. Shan and J. Qu, *J. Appl. Polym. Sci.*, 2017, **134**, 44735–44746.
36 S. Zhu and W. Shi, *Polym. Int.*, 2002, **51**, 223–227.